Integration of enzyme immobilised single-walled carbon nanotube arrays into microfluidic devices for glucose detection

Jingxian Yu*,†, Rudolph Le Roux†, Yunfeng Gu†, Kamran Yunus†, Sinéad Matthews†, Joe G. Shapter* and Adrian C. Fisher†

* School of Chemistry, Physics and Earth Sciences, Flinders University, Bedford Park, SA 5042, Australia
Email: joe.shapter@flinders.edu.au
† Department of Chemical Engineering, University of Cambridge, Cambridge, CB2 3RA, United Kingdom
Email:acf42@cam.ac.uk

***Abstract*—Microfluidic devices for glucose detection have been constructed and developed by integration of glucose oxidase covalently immobilised single-walled carbon nanotube arrays into a poly (dimethylsiloxane)-based microfluidic channel. This microfluidic device was tested for electrochemical glucose detection, and the results showed that the glucose can be detected with a linear response up to a concentration of 5×10^{-3} mol L^{-1}. Because of the small amounts of fluids and enzyme used in microchannels, this approach offers a number of technical advantages, such as portability, shorter analysis time and lower consumption of expensive analytes.**

Keywords-Microfluidic devices; glucose oxidase; carbon nanotube; glucose

I. INTRODUCTION

Glucose sensing is extremely important commercially, since diabetics need to keep control of their blood glucose to prevent either hypoglycaemia or hyperglycaemia. The early sensors tested for ketones in urine, which are indicative of raised blood glucose levels [1]. However the delay in metabolism of glucose to ketone metabolites prevented close monitoring of blood glucose. The big advance in direct measurement of blood glucose came when the enzyme glucose oxidase (GOD) became widely available [2, 3]. Glucose oxidase oxidises glucose to gluconic acid, liberating hydrogen peroxide, which can then be electrochemically [4] and optically [5] detected. The major problem with using the hydrogen peroxide reduction current as an indirect measure of glucose concentration is that oxygen concentration can vary in different samples. The solution to this problem was to realise that oxygen's role only is as an electron shuttle. It has been found that ferrocene and ferrocene compounds (Fc) have good bio-compatibility with GOD [6, 7]. The glucose detection scheme could be now expressed as follows:

$$\text{GOD} + \text{Glucose} \rightleftarrows \text{GOD (ox)} + \text{Gluconic acid}$$

$$\text{GOD}^- + \text{Fc}^+ \rightarrow \text{Fc} + \text{GOD}$$

$$\text{Fc} \rightleftarrows \text{Fc}^+ + e^-$$

Microfluidic techniques offer a number of technical advantages due their ability to manipulate small volumes (10^{-9} to 10^{-18} litres) [8, 9]. In recent studies the use of microreactors to exploit chemical and biochemical reactions have been reported. However, one of the key challenges is to induce an immobilization of reagents and catalysts within these devices providing improved stability and higher sensitivity in chemical analysis [5]. Some researchers have described the immobilization that results from the conjugation of reagents on the inside walls of the flow channel [10]. Others have immobilized enzyme or single strands of DNA on micro-beads in microfluidic device [11].

Carbon nanotubes, with their ability to act as near-perfect conductors of electricity, have been touted as an important building block for nanoscale electronics and biosensors. The traditional approach to fabricating an enzyme/carbon nanotube electrode involves depositing an enzyme layer over the surface of an electrode resulting in an unknown spatial relationship between the redox proteins and the nanotubes [12]. Gooding reported protein electrochemistry using aligned carbon nanotube arrays [13]. The enzymes were covalently attached to the ends of the aligned carbon nanotubes by modifying single walled carbon nanotubes (SWCNTs) onto a cysteamine self-assembled monolayer on gold electrodes. This process provides a simple method for covalently attaching enzymes to carbon nanotubes. Such structures could be incorporated in microfluidic devices to detect biomolecules that interact with a linked enzyme. Integration of microarrays with microfluidic devices can be highly advantageous in terms of portability, shorter analysis time and lower consumption of expensive analytes.

II. MICROFABRICATION

A. Micropatterning

Glass wafers (6×6 cm^2) were treated and cleaned with a piranha solution to remove any organic contaminations and then rinsed thoroughly in Milli-Q water before being blow

dried using a clean supply of nitrogen. The cleaned wafers were then spin coated with a layer of SU-8 photoresist, where the thickness of the photoresist film was controlled by the spin speed and duration. After a pre-baking process, the coated wafers were then exposed to UV-light through a photo mask (Cicuit Graphics) using a mask aligner (MJB3, Karl Suss). The exposed SU8 was then put through a post baking process before being developed to remove the un-exposed regions of the SU8 film, leaving a micropattern of the SU8 structures on the glass wafers. Using a soft lithography approach the raised SU8 features were used as a micromould pattern and were used to cast a microchannel in a PDMS.

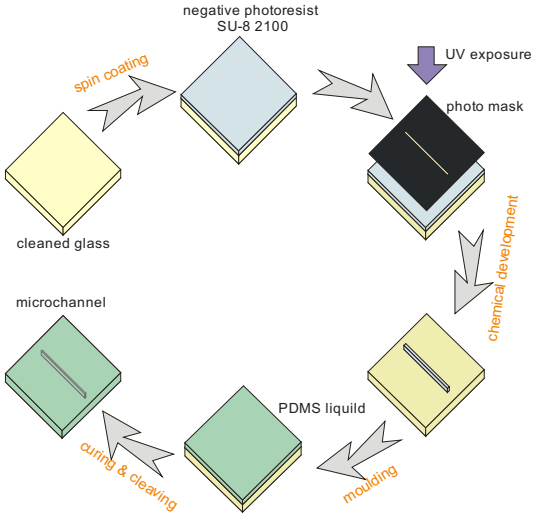

Figure 1. Outline of photoresist micropatterning procedure.

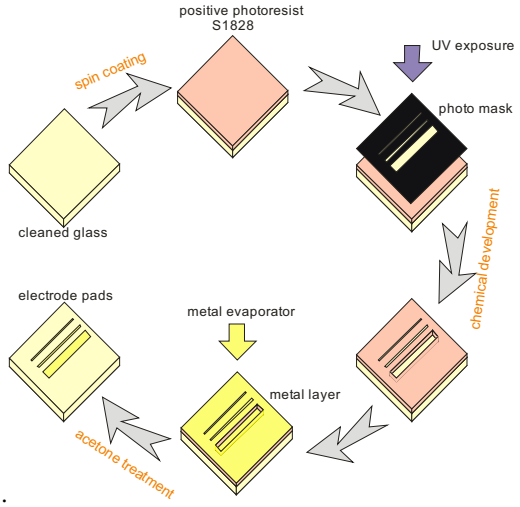

Figure 2. Metal microelectrode deposition procedure.

B. *Microelectrode fabrication*

Using the photolithographic procedure as detailed above, photoresist S1828 was patterned on the surface of the glass wafers. The patterned wafers were then put through a metal coating cycle using a metal evaporator (Edwards Auto 306) to give a titanium/gold film. The coated wafers were then immersed in acetone to lift off the photoresist to reveal the pattern of microelectrodes on the glass wafers.

C. *Immobilisation of enzyme onto electrode band*

Following the procedure outlined by J.J. Gooding [13] and Z. Liu [14, 15], 0.020 g of the 8 hours functionalised single-walled carbon nanotubes (P2-SWCNTs, Carbon Solution, Inc) and 0.100g of dicyclohexylcarbodiimide (DCC, ≥99%, Fluka) were dispersed in 200 mL of N, N-dimethylformamide (DMF, HPLC grade, 99.9+%, Aldrich) by ultrasonication for 5 hours. A clean gold microelectrode band was exposed in a 0.2 mol L^{-1} cysteamine, $NH_2(CH_2)_2SH$ / ethanol solution via a PDMS channel for 5 hours resulting in an amino terminated monolayer being formed. The microelectrodes were then washed with absolute ethanol and dried under nitrogen before being exposed to the carbon nanotube suspension for 12 hours, allowing the amines on the gold surface to form amide bonds with the carbon nanotubes.

The terminal carboxylic acid groups of functionalised carbon nanotubes were activated by exposure to a pH 5.5 phosphate buffer solution (PBS) containing 0.02 mol L^{-1} N-(3-dimethylaminopropyl)-N'-ethylcarbodiimide hydrochloride (EDC, ≥99.0%, Fluka) and 0.05 mol L^{-1} N-hydroxysuccinimid (NHS, 98%, Aldrich) for 1 hour. The activated microelectrode band was rinsed with pH 5.5 PBS buffer solution and immediately placed in pH 5.5 PBS buffer solution with glucose oxidase (490 µg protein mL^{-1}, Type VII from Aspergillus Niger, EC 1.1.3.4, Sigma, UK) for 90 minutes. Microelectrodes with immobilised GOD were rinsed with copious amount of water and used immediately.

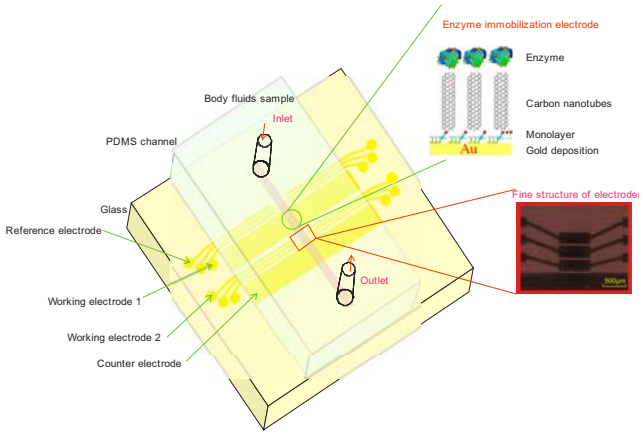

Figure 3. Assembled microfluidic device.

D. *Microfluidic device assembly*

The Polydimethylsiloxane (PDMS) microchannels and the glass microelectrode wafers were then plasma ashed using an oxygen plasma cleaner. The two ashed surfaces were then aligned before being contacted and sealed by heating at 65C for 2 hours. Figure 3 shows a typical image of the assembled microfluidic device.

III. RESULTS AND DISCUSSION

Figure 4(a) shows the linear sweep voltammograms of 0.01 mol L^{-1} phosphate buffer solution (pH = 7.0) containing 100 μmol L^{-1} ferrocenecarboxylic acid and 2×10^{-3} mol L^{-1} D-(+)-glucose at potential scan rate 5 mV s^{-1} by working under bi-potentiostat for different flow rates when no glucose oxidase is present. The potential sweeps on the working electrode 1 started from 0 V for different flow rates, going in the anodic direction. Typically under the flow rate of 0.5 mL min^{-1}, the current response on the working electrode 1 is little at the beginning, nearly zero. However, the current response on the working electrode 2 is at a maximum of about 0.20 μA. After the potential sweep on the working electrode 1 reaches 0.2 V, the current response starts to increase. At the same time, the current on the working electrode 2 goes down. After the potential sweep attains 0.45 V, the current response on the working electrode 1 gets to a maximum, about 0.21 μA, and the current response on the working electrode 2 gets the minimum, about 0.16 μA.

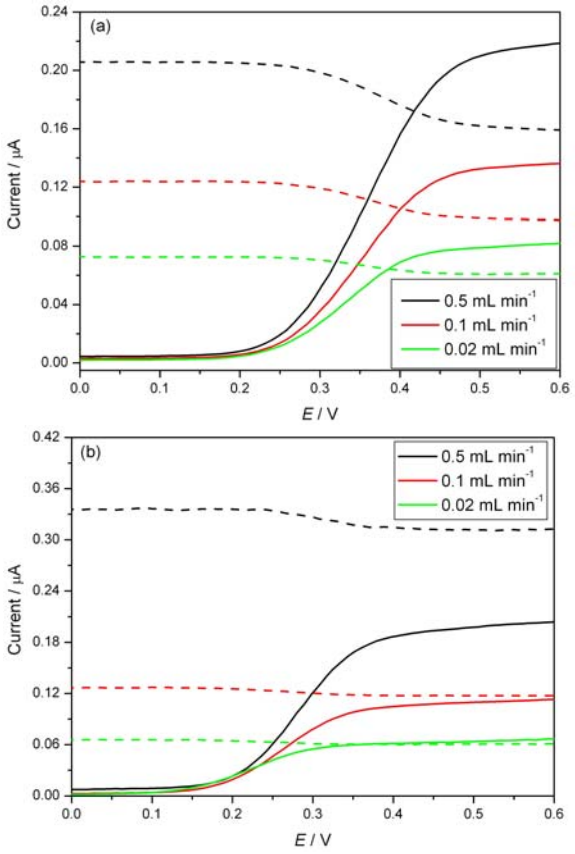

Figure 4. Linear sweep voltammograms of 0.01 mol L^{-1} phosphate buffer solution (pH = 7.0) containing 100 μmol L^{-1} ferrocenecarboxylic acid and 2×10^{-3} mol L^{-1} D-(+)-glucose by working under bi-potentiostat mode for different flow rates when glucose oxidase is (a) absent and (b) present. The potential on working electrode 1 was scanned from 0 to 0.6 V at scan rate 5 mV s^{-1}, and the potential on working electrode 2 was held constant at +0.6 V. Solid line: Current response on the working electrode 1. Dash line: Current response on the working electrode 2.

Figure 4(b) shows the linear sweep voltammograms of 0.01 mol L^{-1} phosphate buffer solution (pH = 7.0) containing 100 μmol L^{-1} ferrocenecarboxylic acid and 2×10^{-3} mol L^{-1} D-(+)-glucose after glucose oxidase is immobilised. Typically under the flow rate of 0.5 mL min^{-1}, the current response on the working electrode 2 is at its maximum at the beginning, about 0.34 μA. After the potential sweep on electrode 1 reaches 0.45 V, the current response on the working electrode 1 gets the maximum, about 0.20 μA. At the same time, the current response on the working electrode 2 gets the minimum, about 0.31 μA. Compared to the current responses when enzyme is absent, the current response on the electrode 1 is similar at the flow rate 0.5 mL min^{-1}, around 0.20 μA. However, the maximum current response on the electrode 2 is much bigger than that when no enzyme is present.

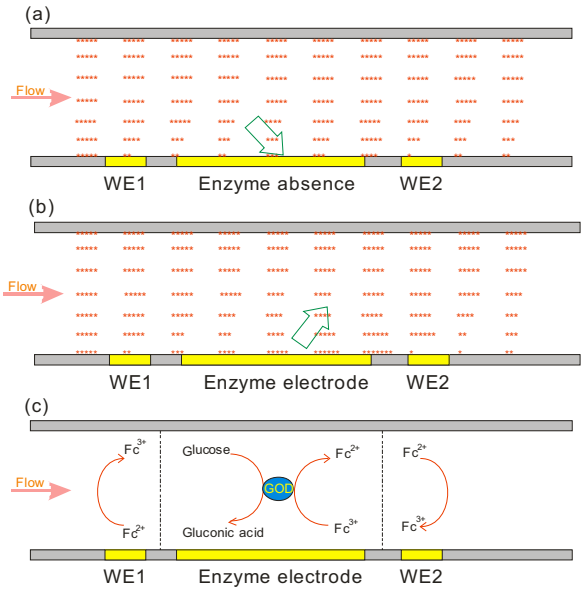

Figure 5. Schematic of the Fc^{2+} concentration profile with position in microchannel when (a) enzyme absence and (b) enzyme presence, and (c) possible chemical reactions in microchannels when enzyme presence. Number of symbol "*" denotes the concentration of Fc^{2+} at the given place. Green arrow indicates the diffusion direction.

Figure 5 shows the schematic of the Fc^{2+} concentration profile with position in microchannel. When no enzyme is present, the electrochemical active ferrocenecarboxylic acid molecules are first oxidised on the working electrode 1, then flow over the working electrode 2. Because of the oxidisation on the working electrode 1, the concentration of Fc^{2+} gets smaller in the laminar layers close to electrode surfaces. At the same time, ferrocenecarboxylic acid molecules diffuse from the far laminar layers to compensate the concentration consumption. If the flow rate is higher, the diffusion distance is shorter before reaching the working electrode 2. In essence, ferrocenecarboxylic acid solution is an equilibrium system between Fc^{2+} and Fc^{3+} ions. When enzyme is present, Fc^{3+} ions can be turned over to Fc^{2+} ions by interaction with glucose under the catalysis of the glucose oxidase. Figure 5(c) shows the possible chemical reactions in microchannels. When the potential sweep starts from 0 V, the surface concentration of Fc^{2+} on electrode 1 does not change because no oxidisation takes place. But the ratio of $Fc^{2+/3+}$ increases in the close

laminar layers when ferrocenecarboxylic acid solution sweeps over the enzyme electrode. So a larger maximum current response on the working electrode 2 can be observed, with an increasing gradient over the flow rate because of the diffusion effects. The higher flow rate is, the thinner the diffusion is, and hence the larger detection current response should be.

Figure 6 shows the variation of maximum current response on the working electrode 2 against the glucose concentration. It can be seen that the variation in current response is reasonably linear up to a glucose concentration of 5×10^{-3} mol L^{-1}, where the square of the correlation coefficient is 0.9868. The linear range could be extended by changing configuration parameters of microfluidic devices. The sensitivity and dynamic range is similar to multilayer enzyme electrode [16] and channel sensor [4] despite the much smaller amount of enzyme immobilized. It reflects the efficient turnover of glucose and ferrocenecarboxylic acid by enzyme electrode in microchannels.

Because of small amounts of fluid (10^{-9} to 10^{-18} litres) and enzyme in microchannels, microfluidic technologies offer a number of technical advantages, such as minimal device size for hand-held instrumentation and point-of-care testing, low production costs per device allowing disposable microfluidic systems, precise volumetric control of samples and reagents leading to higher sensitivities in analytical applications and efficient use of expensive chemical reagents.

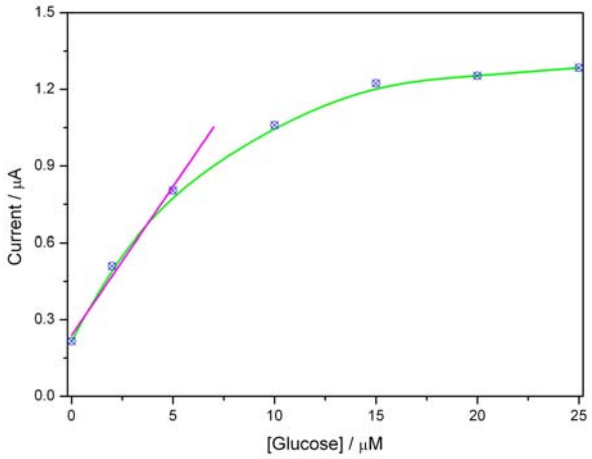

Figure 6. Variation of maximum current response on the working electrode 2 against the glucose concentration.

IV. Conclusions

Microfluidic devices for glucose detection have been constructed and developed by integration of glucose oxidase covalently immobilised single-walled carbon nanotube arrays into a poly (dimethylsiloxane)-based microfluidic channel. The electrochemical results showed that the glucose can be detected with a linear response up to a concentration of 5×10^{-3} mol L^{-1}.

Acknowledgment

J. Yu would like to thank for the financial supports from the ARCNN Overseas Travel Fellowship, ARNAM Student Scholarship for Collaborative Research Support, Flinders University Overseas Traveling Fellowship and Roger Pysden Memorial Fellowship.

References

[1] F. Prisco, A. Picardi, D. Iafusco, R. Lorini, L. Minicucci, M. E. Martinucci, S. Toni, F. Cerutti, I. Rabbone, R. Buzzetti, A. Crino, and P. Pozzilli, "Blood ketone bodies in patients with recent-onset type 1 diabetes (a multicenter study)," *Pediatric Diabetes,* vol. 7, pp. 223-228, Aug 2006.

[2] H. Gunasingham, C. H. Tan, and H. M. Ng, "Pulsed amperometric detection of glucose using a mediated enzyme electrode," *Journal of Electroanalytical Chemistry,* vol. 287, pp. 349-362, Jul 1990.

[3] W. Z. Jia, K. Wang, Z. J. Zhu, H. T. Song, and X. H. Xia, "One-step immobilization of glucose oxidase in a silica matrix on a Pt electrode by an electrochemically induced sol-gel process," *Langmuir,* vol. 23, pp. 11896-11900, Nov 2007.

[4] D. Losic, M. Zhao, J. G. Shapter, and J. J. Gooding, "Which parameters affect the response of the channel biosensor?," *Electroanalysis,* vol. 15, pp. 183-190, Feb 2003.

[5] J. Kim, J. Baek, H. Kim, K. Lee, and S. Lee, "Integration of enzyme immobilized single-walled carbon nanotubes mass into the microfluidic platform and its application for the glucose-detection," *Sensors and Actuators a-Physical,* vol. 128, pp. 7-13, Mar 2006.

[6] M. E. Ghica and C. M. A. Brett, "Development of a carbon film electrode ferrocene-mediated glucose biosensor," *Analytical Letters,* vol. 38, pp. 907-920, 2005.

[7] M. G. Boutelle, L. K. Fellows, and C. Cook, "Enzyme packed-bed system for the online measurement of glucose, glutamate, and lactate in brain microdialysate," *Analytical Chemistry,* vol. 64, pp. 1790-1794, Sep 1992.

[8] F. K. Balagadde, L. C. You, C. L. Hansen, F. H. Arnold, and S. R. Quake, "Long-term monitoring of bacteria undergoing programmed population control in a microchemostat," *Science,* vol. 309, pp. 137-140, Jul 2005.

[9] G. M. Whitesides, "The origins and the future of microfluidics," *Nature,* vol. 442, pp. 368-373, Jul 2006.

[10] T. L. Yang, S. Y. Jung, H. B. Mao, and P. S. Cremer, "Fabrication of phospholipid bilayer-coated microchannels for on-chip immunoassays," *Analytical Chemistry,* vol. 73, pp. 165-169, Jan 2001.

[11] G. H. Seong, W. Zhan, and R. M. Crooks, "Fabrication of microchambers defined by photopolymerized hydrogels and weirs within microfluidic systems: Application to DNA hybridization," *Analytical Chemistry,* vol. 74, pp. 3372-3377, Jul 2002.

[12] J. Q. Liu, A. Chou, W. Rahmat, M. N. Paddon-Row, and J. J. Gooding, "Achieving direct electrical connection to glucose oxidase using aligned single walled carbon nanotube arrays," *Electroanalysis,* vol. 17, pp. 38-46, Jan 2005.

[13] J. J. Gooding, R. Wibowo, J. Q. Liu, W. R. Yang, D. Losic, S. Orbons, F. J. Mearns, J. G. Shapter, and D. B. Hibbert, "Protein electrochemistry using aligned carbon nanotube arrays," *Journal of the American Chemical Society,* vol. 125, pp. 9006-9007, JUL 30 2003.

[14] X. L. Nan, Z. N. Gu, and Z. F. Liu, "Immobilizing shortened single-walled carbon nanotubes (SWNTs) on gold using a surface condensation method," *Journal of Colloid and Interface Science,* vol. 245, pp. 311-318, Jan 2002.

[15] Z. F. Liu, Z. Y. Shen, T. Zhu, S. F. Hou, L. Z. Ying, Z. J. Shi, and Z. N. Gu, "Organizing single-walled carbon nanotubes on gold using a wet chemical self-assembling technique," *Langmuir,* vol. 16, pp. 3569-3573, APR 18 2000.

[16] J. J. Gooding, P. Erokhin, and D. B. Hibbert, "Parameters important in tuning the response of monolayer enzyme electrodes fabricated using self-assembled monolayers of alkanethiols," *Biosensors & Bioelectronics,* vol. 15, pp. 229-239, Aug 2000.